Physica D 50 (1991) 463–477
North-Holland

Experimental demonstration of subtleties in subharmonic intermittency

N. Kreisberg, W.D. McCormick and Harry L. Swinney

Center for Nonlinear Dynamics and the Department of Physics, The University of Texas, Austin, TX 78712, USA

Received 20 August 1990
Accepted 15 February 1991
Communicated by R.M. Westervelt

Experiments on the Belousov–Zhabotinsky reaction in a well-stirred flow reactor elucidate one of the routes to chaos, subharmonic intermittency (type III intermittency). Measurements conducted as a function of two independent control parameters demonstrate how difficult it is in practice to distinguish this route to chaos from subcritical period doubling transitions with similar chaotic time signatures. Necessary criteria for the establishment of a second order (continuous) transition, such as the absence of hysteresis, are discussed in the context of one-dimensional maps.

1. Introduction

Three common routes leading to low dimensional chaos have been well studied: the period doubling cascade, the quasiperiodic or "wrinkled torus" transition, and intermittency [1]. The last route is characterized by regular motion (periodic oscillations), called the laminar phase, which is intermittently disrupted by a short burst of erratic behavior. After a burst the system returns to the regular state until the next episode occurs. Generically, three forms of intermittency are possible for a limit cycle that loses stability, one for each of the allowed co-dimension one bifurcations: saddle node, subcritical period doubling and subcritical secondary Hopf. These bifurcations correspond respectively to the three possible ways in which the floquet exponents governing the stability of the limit cycle can cross the unit circle: $+1$, -1, and complex conjugate pairs [2]. Pomeau and Manneville have termed these transitions to chaos types I, II, and III, respectively [3]. Several physical examples of intermittency associated with the saddle node bifurcation have been observed [4–6], and there has been one report each on observations of intermittency associated with the subcritical period doubling [7] and the subcritical Hopf [8].

The phenomenon of intermittency, as discussed by Pomeau and Manneville [3], involves both local and global dynamics that to a certain degree are independent. A limit cycle loses stability via one of the bifurcations mentioned above at the same time that the global structure of the attractor is such that expanding trajectories leaving the newly unstable orbit are brought back to the vicinity of that orbit. This mechanism, usually called the reinjection process, enables one to treat the dynamics with normal form theory with a minimum of assumptions, as discussed in the next section. Because of this local/global dichotomy, two parameters are typically required to observe a true second order transition to chaos through intermittency. Furthermore, it is essential to use perturbations to establish bistability in a system near subharmonic (type III) intermittency.

A distinction must be made between intermittent dynamics, by which we mean characteristic intermittent behavior with an unstable limit cycle and a reinjection mechanism, and the actual bifurcation sequence – the intermittent transition to chaos. An experiment by Dubois et al. [7] provided convincing evidence for the former. In this paper we examine the transition sequence in more detail. Due to the crucial role of nonlinear terms in controlling the reinjection process, it is not possible to deduce the bifurcation sequence by analyzing only the chaotic regime past the onset of intermittency. Our two-parameter study of the Belousov–Zhabotinsky (BZ) reaction clarifies subtle aspects of this transition sequence. For the following discussion we assume that the intermittency is associated with a subcritical period doubling bifurcation, though much of the discussion applies equally for the forms of intermittency which are associated with saddle–node and secondary Hopf bifurcations (e.g. Tresser et al. [9] give a theoretical treatment of the saddle–node case).

2. Theory

Coincident with the loss of stability of a limit cycle (Floquet multiplier passing through -1 in the case of period doubling) there exists a reinjection mechanism that carries expanding trajectories back to the unstable limit cycle along its stable manifold. The proximity of the point of reinjection to the unstable manifold of the limit cycle completely determines the time a given orbit spends in the laminar phase. This portion of the dynamics is governed by the one-dimensional map that is the normal form associated with period doubling [3]:

$$x_{n+1} = F(x_n) = -(1+\epsilon)x_n + Ax_n^2 + Bx_n^3 + \mathscr{O}(\epsilon^2), \qquad (1)$$

which describes successive intersections of trajectories with a suitably chosen Poincaré surface. As the control parameter ϵ passes through zero, the fixed point at $x=0$ loses stability by way of a period doubling bifurcation. The character of the bifurcation is determined by the nonlinear coefficients A and B: subcritical for $B + A^2 > 0$, supercritical for $B + A^2 < 0$.

In their original paper, Pomeau and Manneville [3] were aware that the phenomenon of intermittency was a result of a delicate interaction between local and global processes in phase space. The global or nonlocal portion of the dynamics, however, has not been treated in the application of normal forms except for two common assumptions: (1) the distribution of reinjection points is uniform about the unstable limit cycle, and (2) the time spent in a chaotic burst is relatively brief compared to the length of the average laminar phase. The first stipulation is important in deriving the statistics of intermittency, such as the distribution of laminar lengths [10, 11] and the scaling laws for Lyapunov exponents [3]. The second assumption is made in calculating the $1/f^{\alpha}$ form of the power spectrum at $\epsilon = 0$ [12]. The connection to critical phenomena is often made by considering the average length of the laminar phase Λ as an order parameter and noting that $1/\Lambda$ grows smoothly from zero as one passes through the transition point.

The interplay of local and global dynamics is best understood in terms of the bifurcation diagrams for subcritical period doubling, as shown in fig. 1. (Similar diagrams are shown in ref. [13] for the forced Duffing equation.) The subharmonic intermittency transition to chaos consists of a second order (continuous) bifurcation between the stable limit cycle and the full attractor that exists *after* the period doubling cascade and reverse-band merging. In fig. 1 the onset of period doubling and the completion of reverse-band merging are labeled PD and BM, respectively. The allowed region of phase space for reinjection is delimited by the extent of the chaotic attractor measure (shaded portions of bifurcation diagram), so that the range of x which falls between the bands of the 2^n-banded chaotic attractor is never visited. If the limit cycle were to lose stability prior to band merging completion (BM), there would either be a small amount of hysteresis, as in fig. 1b, or full hysteresis, as in fig. 1c. The difference lies in whether the 2-band chaotic attractor intersects the basin boundary (dotted line) of the period-one limit cycle twice (b) or not at all (c). These intersections (labeled C_1 and C_2) are crises [14], which signal a transition between bistable and monostable states of the system. Between C_1 and C_2 there exists only one stable attractor – the period one limit cycle – but between C_2 and PD both the 1-cycle and the 2-band attractor are stable, forming a small hysteresis loop; see fig. 1b. In this case the initial appearance of the chaotic attractor just past the onset of subcritical PD contains a significant gap in the distribution of reinjection points around the unstable limit cycle that continuously decreases until BM is reached. Cases (a) and (b) are similar except (b) possesses a small amount of hysteresis and a gap of allowed reinjections around the limit cycle, either of which may be unresolvable in physical systems. Case 1(c) encompasses a whole family of scenarios since the primary period doubling bifurcation could, in principle, occur at any

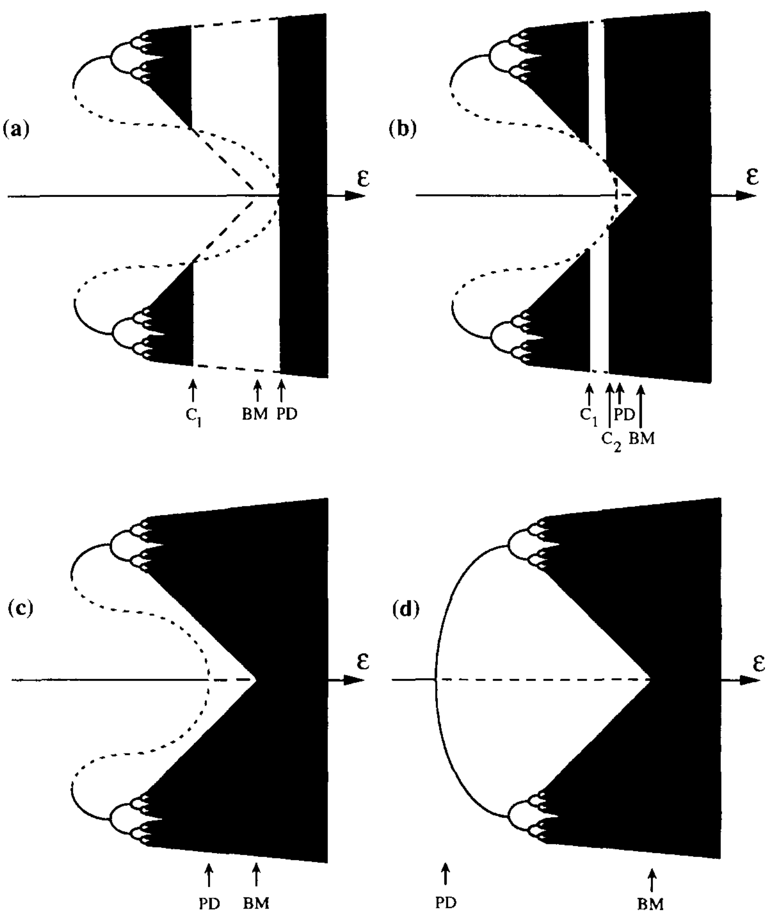

Fig. 1. The schematic bifurcation diagrams in (a)–(c) all yield time series that have the signatures of subharmonic intermittency, but only the sequence in (a) is a continuous (non-hysteretic) transition; the sequences in (b) and (c) have increasing amounts of hysteresis. The same system can exhibit all three sequences (a)–(c), as well as supercritical period doubling (d), for different values of a second bifurcation parameter. The diagrams illustrate the relative positions of the onset of period doubling (PD) and the completion of the band merging (BM) process. C_1 and C_2 indicate the positions of interior crises. The periodic windows in the chaotic regime are omitted for clarity.

point between the 2^n-cycles and 2^n-banded attractors for $n = 1$ to infinity. Sequences in this case, of course, would have varying amounts of hysteresis.

The last case, the supercritical transition, fig. 1d, is included for completeness. Supercritical and subcritical transitions can usually be easily distinguished because experiments typically yield several supercritical doublings of the period (see e.g. ref. [15], table 9.1, p. 29 for a summary of experiments). After the reverse-band merging sequence is completed in the supercritical case, the Floquet multiplier will generally be much less than -1 since the multiplier first leaves the unit circle with the primary period doubling bifurcation. If a reinjection path such as a homoclinic connection still exists at this point in the bifurcation sequence, then very short laminar phases result.

Two distinct properties interact to determine the nature of the transition to chaos: (1) the degree of stability of the limit cycle (magnitude of the floquet multiplier) and (2) the location of the primary period doubling bifurcation point with respect to the rest of the period doubling bifurcation structure. In terms of one-dimensional dynamics, these properties correspond to the slope of the map through the fixed point and the relative height of the unimodal hump, respectively (see fig. 2). For the period doubling bifurcation it is helpful to compose the second iterate of the map $F(x_n)$:

$$x_{n+2} = F^2(x_n) = F(x_{n+1}) = (1 + 2\epsilon)x_n - 2(B + A^2)x_n^3 + \mathscr{O}(\epsilon^2), \qquad (2)$$

where only the lowest order term in ϵ is retained. Note that the quadratic dependence on x has dropped out but that a combination of two nonlinear coefficients A and B control the character of the bifurcation. This point will become important in discussing experiments. As pointed out by Tresser et al. [9], if the peak of the map at the onset of intermittency ($\epsilon = 0$) already exceeds an invariant square constructed from $F^{-2}(x_0^*)$ (dashed squares in fig. 2b), which is the second inverse iterate of the fixed point x_0^*, there is a transition to intermittency without hysteresis. Prior to the transition, the relevant invariant

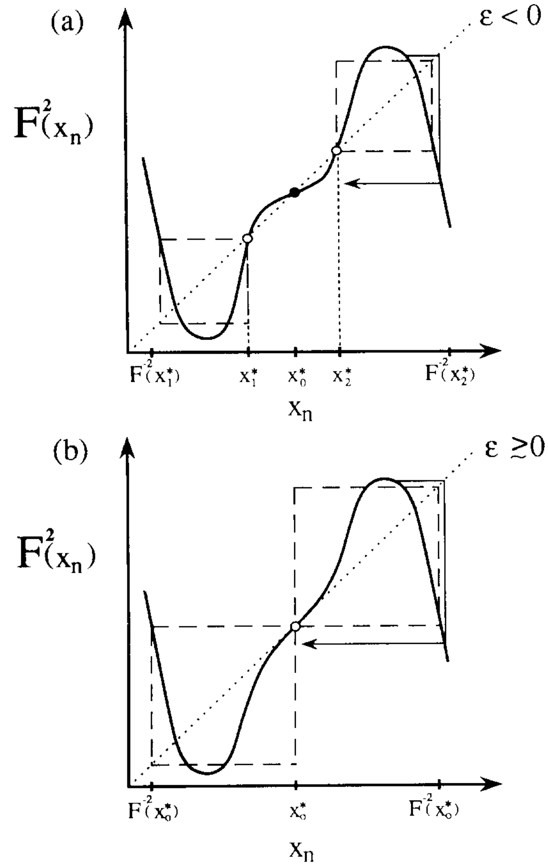

Fig. 2. A second return map illustrates the situation (a) before ($\epsilon < 0$) and (b) just after ($\epsilon \gtrsim 0$) a subcritical period doubling bifurcation with a reinjection process fitting the sequence of fig. 1a. For $\epsilon < 0$, a pair of unstable fixed points, x_1^* and x_2^*, form a period-two cycle such that $x_2^* = F(x_1^*) = F^2(x_2^*)$. The reverse iterates of these unstable fixed points, $F^{-2}(x_1^*)$ and $F^{-2}(x_2^*)$, define invariant squares that govern the existence of hysteresis (dashed squares in (a)). If the extrema of the map exceed these invariant squares, then no hysteresis can exist because iterates of most initial conditions within these intervals will escape into the basin of attraction for the 1-cycle (see example trajectory). Just beyond transition, when $\epsilon \gtrsim 0$ and $F^{2\prime}(x_0^*) \approx (F'(x_0^*))^2 \approx +1$, the unstable fixed points merge with x_0^* causing the invariant squares to coalesce with the invariant squares constructed from x_0^* and $F^{-2}(x_0^*)$; see (b). Solid (open) circles denote stable (unstable) fixed points.

square is determined from the second inverse iteration of the unstable period-two fixed points, x_1^* and x_2^*, where $x_1^* = F(x_2^*) = F^2(x_1^*)$ (dashed squares in fig. 2a). As ϵ approaches zero, the period-two fixed points merge with x_0^* at which point the invariant squares of fig 2a and 2b become identified.

For $\epsilon \leq 0$, x_0^* will be stable, and trajectories which visit regions of the map's maximum (minimum) that lay outside the invariant squares of fig. 2a will be injected below x_2^* (above x_1^*) on the next iteration (see the example trajectory in fig. 2a). Some of these trajectories will always fall into the basin of attraction of x_0^*, the interval $[x_1^*, x_2^*]$, and thereby preclude the possibility for hysteresis. This is an oversimplification because, even if the map exceeds this invariant square, there will exist an infinite set of initial conditions within the intervals $[x_1^*, F^{-2}(x_1^*)]$ and $[x_2^*, F^{-2}(x_2^*)]$ for which all iterates will remain inside this domain. These points, however, define an invariant Cantor set of Lebesgue measure zero and they therefore do not concern us in the context of physical experiments [16].

If, on the contrary, the peak of the map at transition is contained within the invariant square, which occurs when the height of the map varies more slowly than $F'(x_0^*)$, the slope through x_0^*, then there will be hysteresis between chaos and the fixed point. When the system is lowered below the transition, iterates of the map can be "trapped" inside the invariant square at the same time that $|F'(x_0^*)| < 1$. Conceivably, the height of the map could rise fast enough compared to the changing slope that a supercritical period doubling transition to chaos could even be mistaken for a subharmonic intermittency transition. For example, if the period one attractor remained marginally stable (Floquet multiplier near -1) up to the point where a full banded attractor appeared and one used a coarse parameter mesh, one would observe what appeared to be a direct transition from a limit cycle to full-banded chaos. Moreover, since the limit cycle is assumed to be just barely unstable, the length of the laminar phases would be very long on average and would have the misleading appearance of a continuous, second order transition. Thus experiments must be conducted with a fine mesh in control parameter and with external perturbations to clarify the subtle character of the transition. We have conducted such experiments on the BZ reaction.

3. Experimental

3.1. Apparatus

Experiments were carried out in an acrylic well-stirred continuous flow tank reactor, conical in shape with a volume of 8.4 ml (see Coffman et al. [17] for a schematic drawing). To insure that no contaminants were introduced, such as iron from metal pieces, all parts in contact with solutions except for the commercial electrodes were made of either acrylic, teflon, Kel-F or glass. The reactants were fed through the base of the reactor by precision Pharmacia (P-500) or LDC/Milton Roy (MVP series) dual-piston pumps. The long-term stability and reproducibility of these pumps is 1 part in 1000, which is crucial in performing bifurcation studies in chemical systems such as this one. The displaced products were forced up a narrow tube through which the stirrer enters and then drawn off by an aspirator. A synchronous motor stirred a two-bladed glass propeller inside the reactor at 1800 rpm. Temperature was maintained at 28.00 ± 0.02°C by immersing the reactor up to its neck in a thermostated bath.

Four inlets, each 0.8 mm in diameter, were located in the base of the reactor. The chemicals entering the reactor were not premixed. Two of the inlets were usually fed with different concentrations of the same chemical species with the total flow rate held fixed. With computer control of the pump rates, it was a simple matter to achieve this reciprocal variation and maintain independent control over total flow rate and the concentration of a desired species, such as methanol.

3.2. Reagents

Reagent grade chemicals were used exclusively along with distilled and filtered water. A Barnstead Fi-streem glass still (model A1040) and NANOpure filtration system (model D2798) with organic and ion exchange cartridges were used to obtain Type I[#1] reagent grade water. $KBrO_3$ (Baker) was recrystallized twice in distilled water, and malonic acid (Eastern Chemical) was recrystallized three times in combinations of organic solvents [18]: acetone/chloroform (steps I and III) and ethyl acetate (step II). Steps I and III removed organic contaminants while step II was used to remove iron. Ethyl acetate introduced in the second step had to be removed with the last stage of acetone/chloroform recrystallization. The purity of malonic acid is very important in bifurcation studies since impurities such as iron on the ppm level are known to change significantly the dynamics of the BZ reaction [18]. Cerous sulfate (GFS Chemical) and sulfuric acid (Baker) were used without purification.

The mixed-feed concentrations inside the reactor were initially as follows: $[KBrO_3] = 0.1$ M, $[Ce^{+3}] = 0.0017$ M, $[MA] = 0.25$ M, $[H_2SO_4] = 0.2$ M, and $[CH_3OH] = 10^{-4}$ to 10^{-2} M. Sulfuric acid was combined with the cerium feed, while the bromate and malonic acid solutions were fed separately. Solutions were filtered directly into their respective reservoirs and purged of excess air in the process to reduce problems of bubble formation.

Perturbations of the dynamical state were made by direct injections of 4 to 8 μl of 0.01 M Br^- ion and 0.02 M $HBrO_2$ ion solutions into the reactor, producing initial reactor concentrations of the order 10^{-5} M. These ions are known [19] to be important intermediates in the BZ reaction: Br^- is an inhibitory species and $HBrO_2$ is an autocatalytic species. In addition to injections, the standard BZ reaction was subject to a steady state perturbation in the form of methanol (Mallinckrodt) added to the malonic acid feed stream in varying concentrations. Additions of methanol succeeded in producing intermittent dynamics in experiments with purified malonic acid. Noszticzius et al. [18] have suggested that methanol indirectly through oxidized derivatives produces $HBrO_2$, the autocatalytic intermediate.

[#1] The specific resistance of our water initially meets ASTM (American Society for Testing and Materials) Type I standards (> 18 MΩ cm), but resistivity declines to about 2 MΩ cm due to CO_2 diffusion from the air. The water exceeded Type I standards in all other respects.

3.3. Measurements

The reaction was monitored by measuring the emf of an Orion bromide ion specific electrode (model 95-35) with respect to a Sensorex double junction Ag/Ag–Cl reference electrode (model S700RD). Voltages were converted to a TTL pulse train, with frequency $f \propto (V - V_0)$, with V_0 an offset voltage, and sent to a scalar interfaced to a computer. The effective resolution of this digitization was better than 1 part in 10 000. Data were collected at 0.5 and 1.0 Hz sample rates producing 40–80 samples per orbit. Twelve bit analog outputs from the computer were used to control the flow rates of the pumps for automated parameter scans in concentration and flow rate.

4. Results

Experiments in a two-parameter space, residence time and methanol concentration, were conducted to search for a subharmonic intermittency route to chaos. Residence time τ (≡ volume of reactor/flow rate) has been used extensively in flow reactor experiments as a parameter to control the distance from equilibrium. The choice of methanol as a control parameter was suggested by previous experiments [18] which demonstrated that trace amounts (ppm levels) of alcohols or iron in the BZ reagents could significantly alter the bifurcation structure. We have studied as a function of decreasing residence time the first few bifurcations from the region of large relaxation-type oscillations to a region of complex oscillations and chaos [20]. Methanol concentration was varied from $\sim 10^{-4}$ to 10^{-2} M while τ was varied between 3.5 and 5 min.

We observed for increasing methanol concentration that the amplitude and period of the large-amplitude relaxation-type oscillations diminished in the region studied. The primary period doubling bifurcation changes from supercritical to subcritical at a methanol concentration of 2×10^{-3} M. At a concentration of 6.1×10^{-3} M we observed a bifurcation sequence that is within our resolution the subharmonic intermittency route to chaos: a nonhysteretic transition between a period-one limit cycle and an intermittent state with close reinjection to the unstable limit cycle. Due to critical slowing down in the neighborhood of the transition, very long measurements were needed to obtain the asymptotic states. We usually waited ten residence times or more to be reasonably certain of asymptotic behavior. At a residence time of $\tau = 3.8514$ min, a stable limit cycle was observed, which upon lowering τ to 3.850 min became intermittent (fig. 3b). We take a point half way between these parameter settings for the primary bifurcation: $\tau_{PD} = 3.8506$ min. We will refer to the reduced residence time, $\epsilon \equiv (\tau_{PD} - \tau)/\tau_{PD}$; ϵ is negative below the primary period doubling bifurcation, in accordance with eqs. (1) and (2). With a 0.26% decrease in τ we found that the laminar lengths became distinctly shorter; see fig. 3c.

The bistable character of the subcritical period doubling bifurcation was established by perturbing the period-one limit cycle. An injection of 4 μl of 0.02 M bromous acid causes a rapid transition into the period-two basin of attraction, and the system quickly settled down onto the 2-cycle (see fig. 3a), establishing bistability. Lowering ϵ at this point results in a rapid transition back to the 1-cycle when the saddle–node bifurcation is passed.

Evidence for the lack of hysteresis is presented in fig. 3d. While in a state just past the onset of intermittency, as in fig. 3b, the residence time was increased by 0.1% to put the system just below $\epsilon = 0$, and a data file was taken to record the transient behavior. As fig. 3d illustrates, two chaotic episodes were observed before the reinjection into the basin of attraction of the 1-cycle, whereupon the trajectory settles onto the marginally ($\epsilon \approx 0$) stable attractor. As discussed previously, when lowering the control parameter to just below $\epsilon = 0$ in the case of fig. 1a, the trajectory in phase space will spend time in the chaotic state before being reinjected into the attracting basin of the 1-cycle. The time spent in the chaotic state diverges when approaching $\epsilon = 0$ from below [15] due to the decreasing attraction of the 1-cycle. The significant level of noise and the strong subharmonic content is indicative of the proximity to the subcritical period doubling point and of the resulting sensitivity to the ever-present environmental noise.

Fig. 4a shows a one-dimensional second return map constructed from the time series of bromide ion potential in fig. 3b by taking successive amplitude minima of the oscillations and forming pairs of points $[x_n, x_{n+2}]$. This next-amplitude map is equivalent to a particular projection of the Poincaré map which captures all of the essential dynamics of the low dimensional attractor [21]. There is an obvious cubic dependence on x, in agreement with the normal form of eq. (2). Furthermore, a comparison with fig. 2b suggests the absence of any hysteresis because the peak of the map extends above the invariant square defining a stable 2-band attractor. These results are completely consistent with the continuous transition illustrated in fig. 1a, although due to finite experimental resolution, a small amount of hysteresis, as in fig. 1b, can never be completely ruled out.

For comparison, we next present the original results obtained with unpurified malonic acid (Eastern lot #100643), which clearly exhibit intermittent dynamics even though the primary bifurcation is supercritical. A period-one attractor near the onset of period doubling was observed at $\tau = 5.02$ min (fig. 5a), followed by a period-two state at $\tau = 4.98$ min (fig. 5b). No hysteresis was

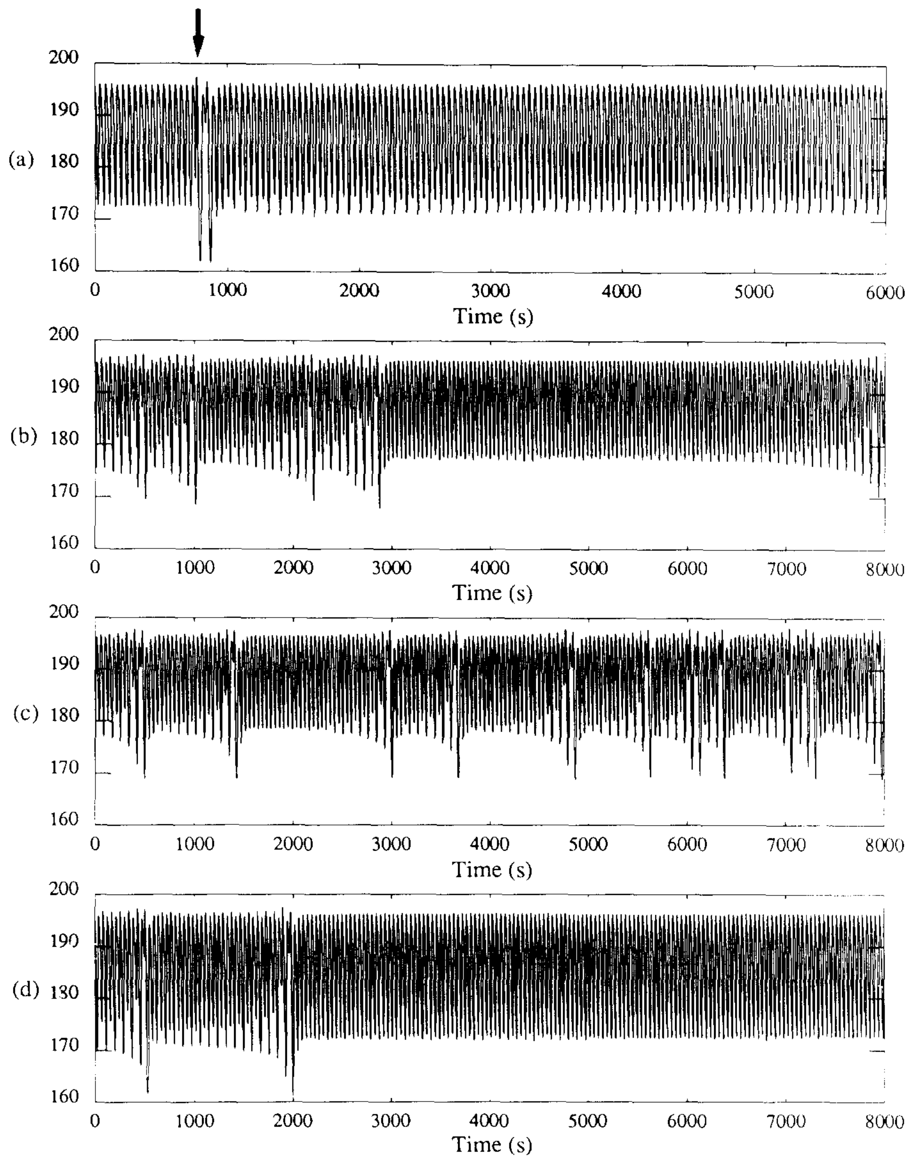

Fig. 3. Time series in bromide ion potential (in mV) illustrating a subcritical period doubling bifurcation leading to intermittency. (a) While on a stable 1-cycle state an injection of 4 μl into the reactor (at the point indicated by the arrow) causes a swift transition into the 2-cycle basin of attraction, where it quickly settles onto the limit cycle ($\epsilon = -3.39 \times 10^{-3}$). (b) The first intermittent regime after the 1-cycle has very long laminar lengths with reinjections directly onto the unstable 1-cycle ($\epsilon = +5.1 \times 10^{-4}$). (c) An increase of 0.14% from the value in (b) in τ leads to a marked shortening of the laminar lengths ($\epsilon = +2.75 \times 10^{-3}$). (d) Increasing τ by 0.05% places the system below the transition point, producing two transient chaotic orbits before a reinjection inside the basin of attraction for the 1-cycle occurs causing rapid settling onto that state ($\epsilon = -5.2 \times 10^{-4}$).

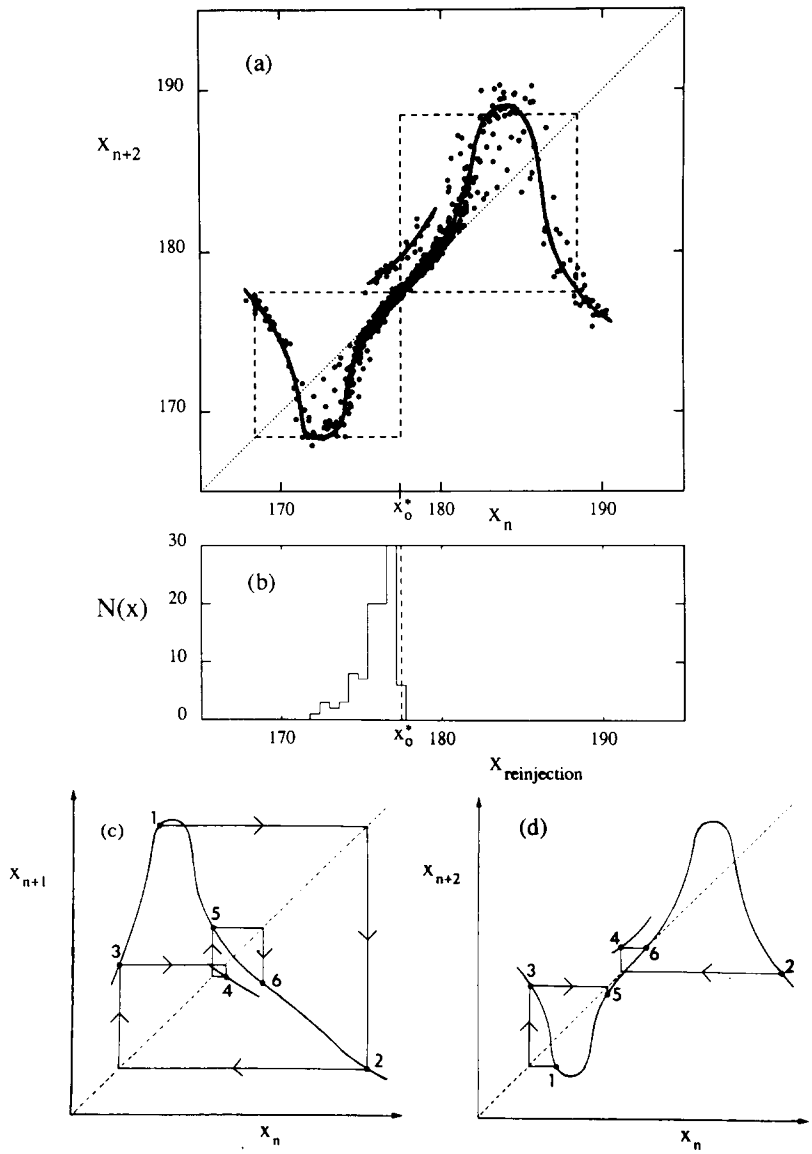

Fig. 4. (a) Second return map constructed from successive amplitude minima of the time series of fig. 3b; the curves are drawn to guide the eye. The cubic inflection at the central unstable fixed point is characteristic of subharmonic intermittency. The absence of an invariant square to "trap" orbits corroborates the lack of hysteresis suggested by the data in fig. 3d. (b) Histogram composed of reinjection points for the data in (a) plus four other data files taken within 0.1% in ϵ of each other. Each histogram was offset to compensate for small differences in the unstable fixed point x_0^*. A total of 80 reinjections was divided into 50 bins of size 0.6. The iteration through a chaotic burst of an initial condition x_1 on the first (c) and second (d) return maps illustrates the reinjection process. The consistent selection of the detached portion of the maps for the fourth iterate creates an asymmetry in the distribution.

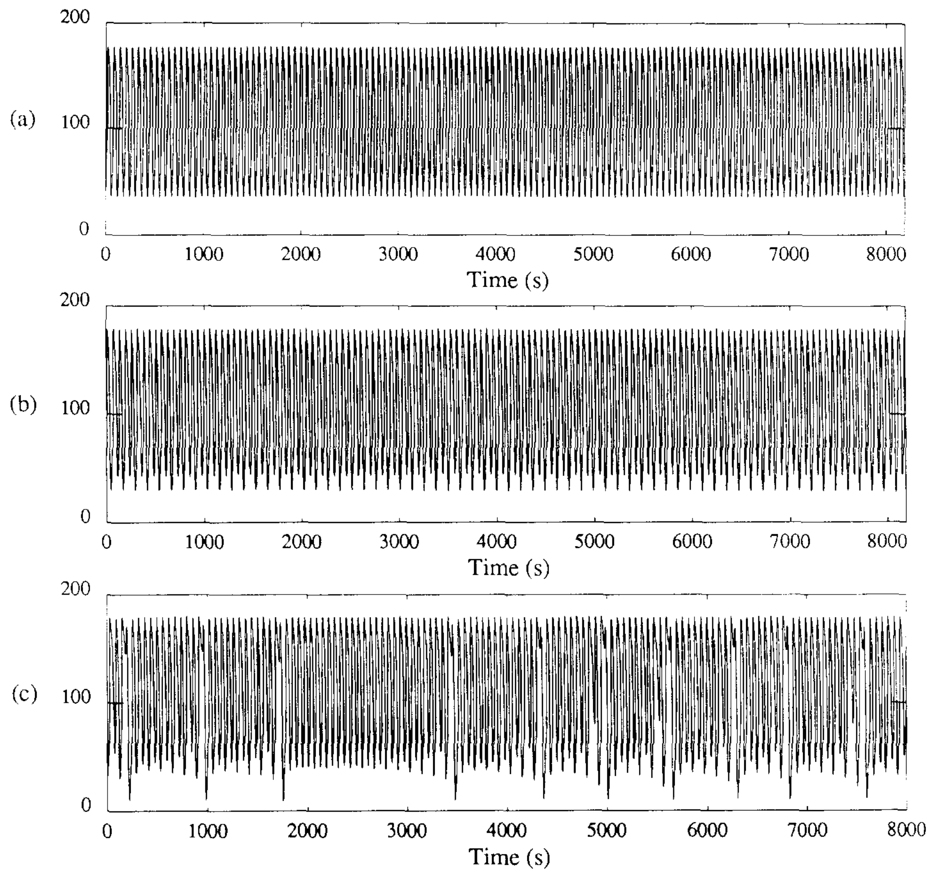

Fig. 5. Time series in bromide ion potential for a supercritical period doubling bifurcation. (a) A period-one limit cycle at $\epsilon = -2.4 \times 10^{-3}$ is followed by (b) a period-two cycle at $\epsilon = +6.6 \times 10^{-3}$ whose subharmonic amplitude is observed to grow continuously from zero with increasing ϵ. (c) At $\epsilon = +2.85 \times 10^{-2}$ an intermittent type of dynamics exists with reinjections directly onto the unstable 1-cycle.

observed to within 0.5%, the experimental parameter mesh. Only transitions between the 1- and 2-cycle were observed for either direction of changing τ. Following the 2-cycle, a state with 2^n oscillations, where $n \approx 2$–3, was observed just prior to chaos, but this state was rarely observed to be stable for more than a couple of periods. At $\tau = 4.87$ min (fig. 5c), an intermittent chaotic state with well-defined laminar phases existed. A reinjection directly onto the unstable 1-cycle can be seen in this segment of the time series, which indicates that the reverse band merging point has been passed. We interpret this transition sequence as being either the case depicted in fig. 1d or 1c. For these observations to agree with the bifurcation diagram in fig. 1c, the point PD must be close (within the 0.5% mesh) to the saddle–node birth of the 2-cycle.

Fig. 6a, the second return map constructed from successive minima of the time series of a state at $\tau = 4.74$ min, shows a clear cubic inflection, and the range of reinjection covers the unstable period-one fixed point with no evident gap around x_0^*. Although this state is 4.4% beyond the primary period doubling bifurcation, the basic structure of this map is the same as that of fig. 4a, including the manner of reinjection considered in the next section. The slope of the supercritical map at the fixed point is greater than unity, indicating that the system is past the transition

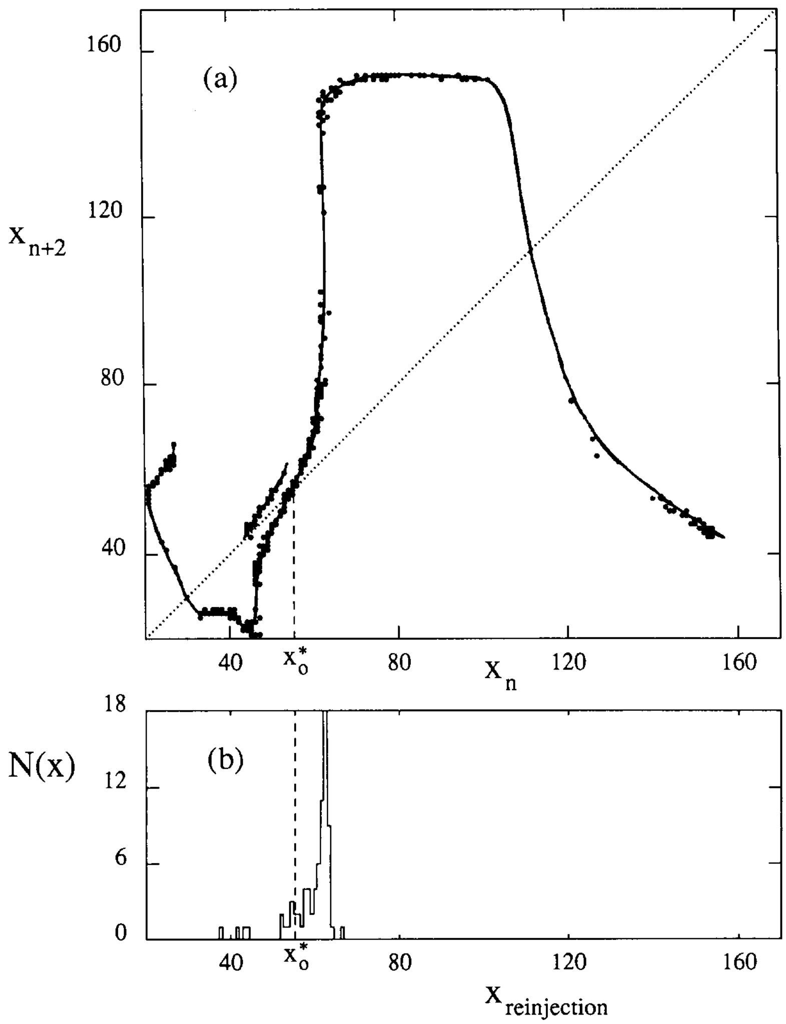

Fig. 6. (a) Second return map constructed from successive amplitude minima of the time series taken at $\epsilon = 0.044$ after the supercritical period doubling sequence to chaos; the curve is drawn to guide the eye to a possible map that would fit these data. This map has a form very similar to the map in fig. 4, including the same double-valued portion around x_0^*, which controls the reinjection process. The cubic inflection is still apparent. (b) Histogram of 75 reinjections for the data in (a), divided into 50 bins of size 0.8, shows the same strongly peaked distribution as with fig. 4b, but here the peak is shifted to the right of x_0^*.

point. Under slightly different conditions, it is possible that the unstable 1-cycle could remain only marginally repelling (i.e., $F'(x_0^*) = -1 - \delta$ with $0 < \delta \ll 1$), creating the potential for arbitrarily long laminar phases and a convincing appearance of a continuous transition. Thus, a supercritical period doubling sequence could ultimately give rise to a chaotic state with the characteristic signature of subharmonic intermittency. The route to chaos, however, would still be that of period doubling, *not* intermittency.

Upon purification of this malonic acid, the intermittent dynamics disappeared along with all complex (or compound) oscillations in the range of τ studied in detail (4–5 min). The period of oscillation observed with the original Eastern malonic acid could be reproduced with the addition of 1.83×10^{-3} M methanol to the purified reagent. Moreover, essentially the same supercritical bifurcation sequence was observed including the intermittent state, so we conclude that methyl alcohol found to be present in the unpurified malonic acid is the essential contaminant contributing to the intermittency dynamics studied in this region.

5. Discussion

We have seen that two criteria must be fulfilled to identify correctly the subharmonic intermittent route to chaos: (1) a nonhysteretic transition between the 1-cycle and full-banded attractor, and (2) the existence of a subcritical branch of states accessible only by perturbation. Beyond these points, one must consider the underlying assumptions of the Pomeau–Manneville theory before one can apply the normal form predictions in a quantitative way. Consider, for instance, the distribution of laminar lengths $P(n)$, as predicted by a direct integration of eq. (1) [22, p. 257]:

$$P(n) \sim e^{-2\epsilon n}/(1 - 4e^{4\epsilon n})^{3/2}, \qquad (3)$$

where n is the number of oscillations per laminar phase. This result assumes that there exists a uniform (white noise) distribution of reinjections about x_0^*. In our chaotic signal, the distinction between the laminar phase and a chaotic burst is not difficult to make (see fig. 7). The amplitude of oscillations varies smoothly up to the appearance of a small amplitude oscillation which is then always followed by two more orbits of the attractor before being reinjected near the unstable fixed point. In fig. 7 an excerpt of the time series of fig. 4b illustrates the characteristic pattern for the chaotic burst. The first three oscillations of a burst are numbered if and only if the fourth oscillation can be considered a reinjection point (labeled "R"). The reinjection point is taken to be the first oscillation (following a chaotic burst) that lies near the unstable period-one fixed point.

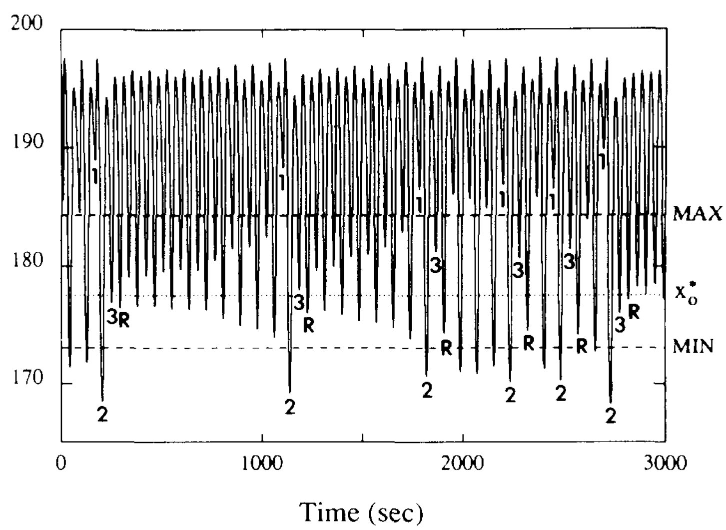

Fig. 7. A short excerpt from the time series in fig. 3b illustrates the robustness of the definition of a chaotic burst, with the reinjection point (labeled "R") always following three characteristic oscillations (numbered 1–3): the first minimum above the threshold MAX, the second below the threshold MIN, and the third between MAX and MIN. Only those sequences of oscillations which have this pattern will produce a reinjection near x_0^*. The minima numbered "3" correspond to the detached island of points in the return maps of figs. 4c, 4d.

By defining a maximum, MAX, and minimum, MIN, value for x, as shown in fig. 7, a trivial algorithm may be established to automatically select the reinjection points $x_{\text{reinjection}}$ from an intermittent time series. Thus, a chaotic episode in nearly every instance consists of just three oscillations, and for ϵ near 0 the laminar phase is nearly always much longer.

A histogram of reinjection points was constructed (see fig. 4b) from the time series of fig. 3b in addition to four other chaotic data sets all taken within 0.1% in ϵ of each other. This composite histogram was used to increase the available statistics to compensate for the long laminar lengths and the relatively few reinjections occurring in each data file. To account for the small dependence of x_0^* on τ, the individual histograms were normalized to a common value of x_0^*; the x_0^* values differed by less than 1%. For each file, x_0^* was found by averaging an even number of minima from a laminar section of the time series corresponding to a close reinjection. For small deviations from x_0^*, the alternating minima depart symmetrically from the unstable fixed point, which insures a reliable estimate for x_0^*.

The observed reinjection process fails to provide a uniform reinjection around x_0^*, as shown in the histogram of reinjection points. Note that in addition to the peaked distribution, no reinjections to the right of the fixed point $(x > x_0^*)$ occur. To understand how this striking asymmetry arises, one must consider the reinjection mechanism in more detail. The attractor can be treated as a single-valued function close to x_0^* and along the left and right tails of the map, from which the reinjection points originate. A small region around x_0^* is clearly seen to be double-valued with a small detached line of points present just above the map in this region. It is this segment that dominates the reinjection process for the attractor. A similar effect was observed with the reinjection histogram for the supercritical case (see fig. 6b). Using a single data file of 75 points, a distribution was obtained possessing the same general shape as that of fig. 4b, but with the narrow peak falling to the right of x_0^*. The position of reinjection histogram peaks was found to depend mostly on methanol concentration and to a lesser extent on ϵ.

Figs. 4c and 4d show a typical trajectory of a chaotic burst as iterated in the first and second return maps, respectively, of the time series of fig. 3b. For the purposes of this discussion the maps are assumed to be one-dimensional everywhere except for the small double-valued region. Whether due to experimental noise or an underlying multi-leaved structure, the scatter about the extrema in the map of fig. 4a does not affect the reinjection process controlled by the tails of the map, which are well approximated by single-valued functions. In the first return map, the isolated portion of the map below x_0^* corresponds to the last oscillation of the chaotic episode just prior to reinjection; this part is visited by orbits originating from the left tail of the map. In the case of the second return map, this line of points gets mapped above x_0^* and becomes the F^2 image of the right side tail. Beginning with the initial condition x_1 near the extrema of the maps, we find that the first two mapped images, $x_2 = F(x_1)$ and $x_3 = F^2(x_1)$, are found deterministically, but that x_4 involves a decision as to whether to go up or down in the double-valued region. After being reinjected onto the unstable manifold of x_0^*, x_5 starts the spiraling out from x_0^* through x_6 and successive iterates until the next burst occurs. The fact that the detached line of points is always selected and that it only falls below (above) x_0^* in the first (second) return map insures that the reinjection onto the unstable manifold of x_0^* is one-sided as well. The proximity of this piece of the map to x_0^* may be due to the existence of a fold in the attractor or of a projection effect in constructing the return maps.

At greater values of methanol concentration (e.g. at 0.0072 M), we observed that the chaotic state near onset possessed a dominant period-five character, suggesting that the primary period doubling bifurcation was occurring near a periodic window within the chaotic region. Indeed, the symbolic dynamics code for the corresponding periodic state was RLR^2 [23], corresponding to the first broad window in the U-sequence. One might naturally suspect that the distribution of reinjections would be influenced by the presence of nearby periodic windows. Indeed, broader distributions were generally observed for chaotic states closer to the 5-cycle window. (The influence of unstable orbits, or saddle points, on chaotic attractors has become of recent interest as a way to measure Lyapunov exponents and to estimate topological entropies [24, 25]. See ref. [25] for an example applied to this particular chaotic BZ state.)

The present experiment is similar to previous numerical experiments [11, 13, 26, 27] which have exhibited intermittency with nonuniform distributions of reinjections points; therefore, the derivation of $P(n)$ must be reconsidered to incorporate the nonuniformity of each specific case. This correction has been performed numerically by Richetti et al. [11, 26] in the case of intermittency associated with the subcritical Hopf bifurcation (type II) in which the distribution of reinjection points fell nonuniformly on a one-dimensional curve rather than a uniform disc. They found that the observed distribution of laminar lengths could be successfully described when this numerical correction was employed. Although all of the observed reinjection distributions in our experiments were of the same form with only the position of the peak changing with methanol concentration, insufficient data made this numerical approach infeasible in our experiment. Given the sharply peaked histograms observed as in fig. 4b, however, we may conclude that agreement with eq. (3) would be unlikely. The scaling law for Lyapunov exponents appears also to rely strongly on the reinjection distribution [27].

In this paper we have discussed the criteria that must be fulfilled to establish a true second order transition to chaos through subharmonic intermittency. We have presented evidence for such a transition in our system: a bistable region between the 1- and 2-cycles and a transition to intermittency without hysteresis. Similar results have been obtained by Richetti [28] in numerical simulations of a 7-variable chemical model that has been shown to qualitatively reproduce a wealth of dynamical behavior seen in BZ experiments [29]. In addition to a true continuous transition to chaos through subharmonic intermittency, this model exhibits the misleading situation of intermittent dynamics following a supercritical period doubling bifurcation like that which we observed.

Finally, we emphasize the necessity of having two or more control parameters to resolve a transition to chaos such as this one in which independent control over local and global properties of the system is required. To insure a subcritical period doubling bifurcation, two nonlinear coefficients (A and B of eq. (1)) must be adjusted independently of the primary control parameter ϵ. This requirement explains, in part, why this transition to chaos has been rarely observed.

Acknowledgements

We thank Alain Arneodo for extensive helpful comments, and Philippe Richetti, John Ringland, and Zoltan Noszticzius for helpful discussions. This work was supported by the Department of Energy Office of Basic Energy Sciences and the Robert A. Welch Foundation (Grant F-805).

References

[1] J.-P. Eckmann, Rev. Mod. Phys. 53 (1981) 643.
[2] G. Iooss and D.D. Joseph, Elementary Stability and Bifurcation Theory (Springer, Berlin, 1981).
[3] Y. Pomeau and P. Manneville, Commun. Math. Phys. 74 (1980) 189.
[4] P. Bergé, M. Dubois, P. Manneville, and Y. Pomeau, Phys. Rev. Lett. 51 (1983) 1446.

[5] P.S. Lindsay, Phys. Rev. Lett. 47 (1981) 1349; J. Testa, J. Peréz and C. Jeffries, Phys. Rev. Lett. 48 (1982) 714.
[6] Y. Pomeau, J.C. Roux, A. Rossi, S. Bachelart and C. Vidal, J. Phys. (Paris) Lett. 42 (1981) L271.
[7] M. Dubois, M.A. Rubio and P. Bergé, Phys. Rev. Lett. 51 (1983) 1446.
[8] J.Y. Huang and J.J. Kim, Phys. Rev. A36 (1986) 1495.
[9] C. Tresser, P. Coullet, and A. Arneodo, J. Phys. (Paris) Lett. 41 (1980) L243.
[10] J.E. Hirsh, M. Nauenberg and D.J. Scalapino, Phys. Lett. A 87 (1982) 391; J.E. Hirsh, B.A. Huberman and D.J. Scalapino, Phys. Rev. A 25 (1982) 519.
[11] F. Argoul, A. Arneodo and P. Richetti, J. Phys. (France) 49 (1988) 767.
[12] A. Ben-Mizrachi, I. Procaccia, N. Rosenberg, A. Schmidt and H.G. Schuster, Phys. Rev. A 31 (1985) 1830.
[13] H. Bunz, H. Ohno and H. Haken, Z. Phys. B 56 (1984) 345.
[14] C. Grebogi, E. Ott, and J.A. Yorke, Phys. Rev. Lett. 48 (1982) 1507; Physica D 7 (1983) 181.
[15] P. Cvitanović, Universality in Chaos (Hilger, Bristol, 1984).
[16] A. Arneodo, private communication (1990).
[17] K.G. Coffman, W.D. McCormick, Z. Noszticzius, R.H. Simoyi and H.L. Swinney, J. Chem. Phys. 86 (1987) 119.
[18] Z. Noszticzius, W.D. McCormick and H.L. Swinney, J. Phys. Chem. 91 (1987) 5129 and J. Phys. Chem. 93 (1989) 2796.
[19] R.J. Field, E. Korös and R.M. Noyes, J. Am. Chem. Soc. 94 (1972) 8649.
[20] M. Kilgore, Ph.D. Dissertation, University of Texas at Austin (1986).
[21] N. Kreisberg, Ph.D. Dissertation, University of Texas at Austin (1991).
[22] P. Bergé, Y. Pomeau and C. Vidal, Order within Chaos (Wiley, New York, 1986).
[23] M. Metropolis, M.L. Stein and P.R. Stein, J. Combinatorial Theory (A) 15 (1973) 25.
[24] D. Auerback, P. Cvitanović, J.-P. Eckmann, G.H. Gunaratne and I. Procaccia, Phys. Rev. Lett. 58 (1987) 2387.
[25] D. P. Lathrop and E.J. Kostelich, Phys, Rev. A 40 (1989) 4028; in: Measures of Complexity and Chaos, eds. N.D. Abraham, A. Albano, A. Passamante and P.E. Rapp (Plenum, New York, 1990).
[26] P. Richetti, F. Argoul, and A. Arneodo, Phys. Rev. A 34 (1986) 726.
[27] G. Mayer-Kress and H. Haken, Physica D 10 (1984) 329; in: Proceedings of the 1982 Conference on Dynamical Systems and Chaos, ed. L. Garrido, Springer Lecture Notes in Physics, No. 179 (Springer, Berlin, 1983) p. 237.
[28] P. Richetti, Thèse, Université de Bordeaux (1987).
[29] F. Argoul, A. Arneodo, P. Richetti and J.C. Roux, J. Chem. Phys. 86 (1987) 3325.